AIP | Journal of Applied Physics

Magnetic properties of Sm-Co thin films grown on MgO(100) deposited from a single alloy target

T. G. A. Verhagen, D. B. Boltje, J. M. van Ruitenbeek, and J. Aarts

Citation: Journal of Applied Physics **116**, 053903 (2014); doi: 10.1063/1.4890227
View online: http://dx.doi.org/10.1063/1.4890227
View Table of Contents: http://scitation.aip.org/content/aip/journal/jap/116/5?ver=pdfcov
Published by the AIP Publishing

Magnetic properties of Sm-Co thin films grown on MgO(100) deposited from a single alloy target

T. G. A. Verhagen, D. B. Boltje, J. M. van Ruitenbeek, and J. Aarts[a)]
Huygens-Kamerlingh Onnes Laboratorium, Universiteit Leiden, P.O. Box 9504, 2300 RA Leiden, The Netherlands

(Received 2 March 2014; accepted 2 July 2014; published online 1 August 2014)

We have grown epitaxial Sm-Co thin films by sputter deposition from a single alloy target with a nominal $SmCo_5$ composition on Cr(100)-buffered MgO(100) single-crystal substrates. By varying the Ar gas pressure, we can change the composition of the film from a $SmCo_5$-like to a Sm_2Co_7-like phase. The composition, crystal structure, morphology, and magnetic properties of these films have been determined using Rutherford Backscattering, X-ray diffraction, and magnetization measurements. We find that we can grow films with, at room temperature, coercive fields as high as 3.3 T, but with a remanent magnetization which is lower than can be expected from the texturing. This appears to be due to the Sm content of the films, which is higher than expected from the content of the target, even at the lowest possible sputtering pressures. Moreover, we find relatively large variations of film properties using targets of nominally the same composition. At low temperatures, the coercive fields increase, as expected for these hard magnets, but in the magnetization, we observe a strong background signal from the paramagnetic impurities in the MgO substrates.
 [http://dx.doi.org/10.1063/1.4890227]

I. INTRODUCTION

Modern permanent magnetic materials, such as $SmCo_5$ and $NdFe_{14}B$, are based on intermetallic compounds of rare-earth and 3d transition metals. Sm-Co intermetallics are hard magnetic materials with a high coercive field and a high uniaxial magnetocrystalline anisotropy, where the easy axis is aligned along the crystallographic *c*-axis. Since the 1970s/1980s many groups investigated the properties of Sm-Co crystals and thin films. The control over the composition and the crystallographic texture are the key parameters to obtain thin films with the desired hard magnetic properties. These properties are interesting from both a technical and a fundamental point of view. The further miniaturization of magnetic microelectromechanical systems (MEMS)[1] can benefit from the controlled growth of such films, but also the combinations between a hard magnet like $SmCo_5$ with soft magnets[2] or superconductors[3] can lead to interesting and useful magnetic configurations.

Generally, one of the underlying problems is the complexity of the Sm-Co phase diagram,[4] in which, on the Co-rich side, the compounds Sm_2Co_{17} (11 at. % Sm), $SmCo_5$ (17 at. % Sm), Sm_5Co_{19} (21 at. % Sm), and Sm_2Co_7 (22 at. % Sm) all exist; with the note that $SmCo_5$ actually is a metastable compound. The connection between composition and magnetic properties is therefore not trivial. Fortunately, high coercive fields can be found over a range of compositions, basically because grain size and grain texture have a strong bearing on this property. The hexagonal crystal structures of the Sm-Co compounds are strongly uniaxial in nature, with the magnetic easy axis along the *c*-axis. To have high coercive fields in the film plane, the *c*-axis of the film should therefore be in-plane. In the last years, recipes have been developed to grow films with the desired hard magnetic properties in different ways. One route is to grow epitaxial thin films. Epitaxial growth can be obtained by using MgO(100), MgO(110), Si(100), or Al_2O_3(0001) single crystals, commonly in combination with a chromium buffer layer in order to promote the correct texture. Growing Sm-Co films on four-fold symmetric MgO(100) substrates results in the epitaxial relation Sm-Co(11$\bar{2}$0)[0001]//Cr(001)[110]//MgO(001)[100]. In this case, the Sm-Co grains are equally distributed along the two orthogonal in-plane directions. Growing on MgO(110) can lead to a Cr(211) buffer and a single orientation of the Sm-Co *c*-axis.[5] Sm-Co films can also be deposited on a glass substrate. Growing on glass results in very small crystallites in a disordered structure, and yields large coercive fields with high remanence.[6]

Thin Sm-Co films are mostly grown using pulsed-laser deposition (PLD)[7–9] or sputter deposition[6,10,11] using two single elemental targets, Sm and Co. By tuning the sputter power of both sources and the pulse ratio by PLD, it is possible to grow thin films with a Sm composition in the desired range. However, for various applications, growing Sm-Co thin films from alloy targets is a desirable option since only one deposition source is needed. Still, as far as we know, relatively few groups[12–20] have reported on the growth of Sm-Co thin films from single alloy targets. The purpose of this work is to show what the properties are of such films, grown on MgO(100), and in a range of pressures. In order to offer a reference frame for our results, we start with a paragraph outlining what has been achieved earlier in terms of coercive fields and saturation magnetization or remanence. We then present experimental details of our work, results of the measurements, and a discussion.

II. SINGLE ALLOY TARGETS; PREVIOUS RESULTS

It is useful to compare results from single target growth to typical results from multiple targets. Without being

[a)]Electronic mail: aarts@physics.leidenuniv.nl

exhaustive, PLD growth using multiple targets on Cr-buffered MgO(100) and MgO(110) was discussed by Singh *et al.*[5,7] In the first case, the more or less equal distribution of grain axes along the two in-plane directions leads to a remanent field $\mu_0 M_r$ of about 0.5 T when measuring along MgO(100), as can be expected from the saturation magnetization $\mu_0 M_s$, which is about 1.1 T for $SmCo_5$. The room temperature coercive field $\mu_0 H_c$ was 2.4 T in this case. For growth on MgO(110) these numbers are $\mu_0 M_r = 0.9$ T (due to a highly uniaxial grain distribution) and $\mu_0 H_c = 3$ T, respectively. Sputter growth on Cr-buffered MgO(100) from multiple targets was performed, among others, by Fullerton *et al.*[21] Using a pressure of 5×10^{-3} mbar, they reported square magnetization loops with $\mu_0 H_c = 3.4$ T for a 30 nm film (decreasing to 1.2 T at 450 nm) but did not give values for M_s or M_r.

For single alloy targets, somewhat surprisingly, no work has been reported using MgO substrates, probably since coercive fields of the order of a Tesla do not require such a substrate. Also, a mixture of Co, Fe, Cu, and Zr was often used rather than pure Co in order to enhance coercivity. One parameter which did vary in the different studies is the sputtering pressure, which will be noted in units 10^{-3} mbar for easy comparison. A summary of the results, where we confine ourselves to processes without post-annealing, are as follows.

Cadieu[12] reported on sputtering thin films using $Sm_2(Co,Fe,Zr,Cu)_{17}$ and $SmCo_5$ targets on Al_2O_3 substrates with a high sputter background pressure (80×10^{-3} mbar), so that the sputtered atoms were thermalized when they arrive onto the substrate and support the growth of large crystallites. For $SmCo_5$, he found $\mu_0 H_c = 2.4$ T and $\mu_0 M_r = 0.9$ T for a 3 μm thick film with a (110) texture. In a different publication,[20] he showed that with a varying sputter gas pressure between 20×10^{-3} mbar and 170×10^{-3} mbar and different sputter gasses (Ar, Xe, and ArXe), it is possible to vary the Sm concentration of the film from a Sm atomic percentage of about 12 at. % to 16 at. %. These films have a typical coercive field of 0.7 T and a remanent magnetization of 0.8 T.

Neu and Shaheen[13] studied the Co-rich part of the Sm-Co phase diagram. Sm-(CoFeCuZr) films were grown by cosputtering $Sm(Co,Fe,Cu,Zr)_7$ and $SmCo_5$ targets on Al_2O_3 substrates. They varied the sputter background pressure in the range of 80–130×10^{-3} mbar. The magnetic properties of these Sm-Co films grown at a constant pressure show a smooth increase in the coercive field when the Sm concentration is increased from 15 at. % to 18.5 at. % (with 16.7 at. % corresponding to $SmCo_5$). The remanent magnetization shows a smooth decrease, connected to the reduced amount of (Co,Fe). When the sputter background pressure is decreased from 110×10^{-3} mbar to 80×10^{-3} mbar, a clear increase in the coercive field and decrease in the remanent magnetization was observed, connected to a higher amount of Cu. The Sm(Co,Fe,Cu,Zr) film that contained 15.8 at. % Sm and was grown at 80×10^{-3} mbar had a coercive field of 0.7 T and a remanent magnetization of 0.8 T.

Speliotis and Niarchos[16] sputtered Sm-Co films on Si substrates from an alloy target with 18 at. % Sm. They discussed the magnetic properties of the Sm-Co films, when the sputter background pressure was varied between 24×10^{-3} mbar and 32×10^{-3} mbar. Again, when increasing the Sm concentration from 11 at. % to 17 at. %, the remanent magnetization decreases and the coercive field increases. The Sm-Co film that contained 15 at. % Sm had a coercive field of 1.5 T and a remanent magnetization of 0.7 T. Summarizing, sputtering from single alloy targets has primarily been studied using Si or Al_2O_3 substrates under various conditions of pressure. The films typically show coercive field of the order 0.7 T (and a maximum reported value of 2.4 T), and remanent fields of the order of 0.7 T–0.8 T, as can be expected from the texturing. In our work, we use a $SmCo_5$ alloy target and MgO(001) single crystal substrates with a Cr buffer layer, and grow films in an Argon pressure range between 1.5×10^{-3} and 12.5×10^{-3} mbar. We are able to vary the Sm content of the films with pressure between 21 at. % Sm and 26.5 at. % Sm. At room temperature, we find typical values for $\mu_0 M_r$ of 0.4 T, somewhat lower than the above results; and values for $\mu_0 H_c$ up to 3.3 T.

III. EXPERIMENT

The Sm-Co films were deposited in a UHV chamber (base pressure 1×10^{-9} mbar) using DC magnetron sputter deposition with argon as plasma from a commercially obtained alloy target with a nominal composition of $SmCo_5$ (3 N). A rotating sample holder was used. The deposition rate was measured by X-ray reflectivity (XRR) using Cu-Kα radiation. The composition of the target was subsequently measured by an inductively couple plasma (ICP) method, and was found to be $SmCo_{4.56(5)}$, containing 18% Sm rather than 16.7%.

Films were deposited on 500 μm thick MgO(100) single crystal substrates on which a 100 nm thick Cr buffer layer was first deposited at 250 °C in an Ar pressure of 1.5×10^{-3} mbar. All Sm-Co films were approximately 100 nm thick and were grown at 450 °C with an Ar pressure varying between 1.5×10^{-3} mbar and 12.5×10^{-3} mbar. Afterwards, a 10 nm thick Cr layer was deposited at 450 °C as a protection layer.

The actual film composition and thickness were determined using Rutherford backscattering (RBS). The structural quality of the film was measured with θ–2θ X-ray diffractometry (XRD) using Cu-Kα radiation, where the MgO substrate peak was measured as a reference for the angle, by using an extra Cu-absorber to decrease the intensity. The morphology of the films was characterized by atomic force microscopy (AFM) in tapping mode. Magnetization measurements were performed in-plane (along a MgO(100) direction lying in the substrate plane) and out-of-plane (along the MgO(001) direction) in a SQUID-based magnetometer (MPMS 5S from Quantum Design) in fields up to 5 T. For the magnetization measurements, the substrates were cut in pieces of approximately $10 \times 4\,mm^2$. As a reference, a MgO(100) substrate was measured, and also a MgO(100) substrate with a 100 nm Cr film protected with 30 nm Cu. Electron paramagnetic resonance (EPR) spectra were measured at room temperature using a Bruker EMX plus X-band spectrometer in a TE_{011} cavity with 100 kHz modulation frequency and 0.1 mT modulation amplitude.

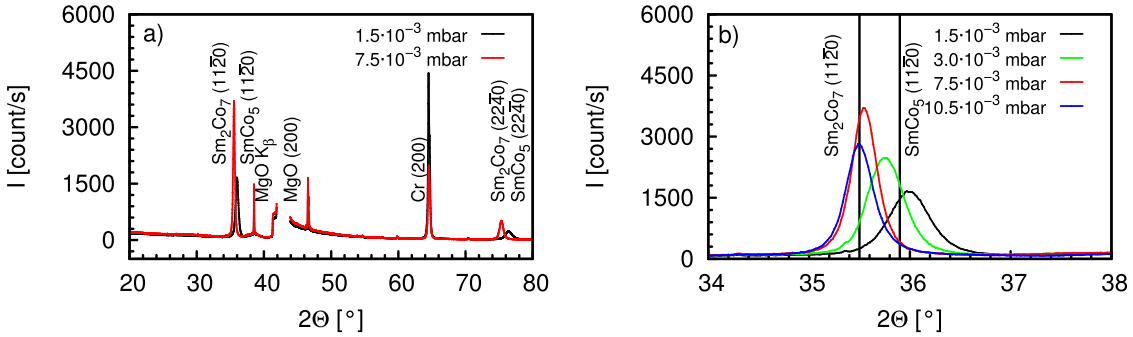

FIG. 1. (a) X-ray diffraction pattern (θ-2θ scan) of Sm-Co films grown from a Sm-Co alloy target on a Cr/MgO(100) substrate with two different sputter gas pressures, as indicated. (b) shows the region around the Sm-Co(11–20) peak, where the two vertical lines indicate the reflection of bulk crystalline Sm_2Co_7 (left) and $SmCo_5$ (right). Four samples are shown, grown at (from right lo left), 1.5 (black), 3.0 (green), 7.5 (red), and 10.5×10^{-3} mbar (blue).

IV. RESULTS

A. Composition and morphology

Figure 1(a) shows the XRD scans of films grown at 1.5×10^{-3} mbar ($SmCo_5$-like) and 7.5×10^{-3} mbar (Sm_2Co_7-like), respectively. The observed peaks are labeled as reflections of Sm-Co, MgO, and Cr. Due to the thickness and high crystallinity, also the K_β peak of the MgO substrate is visible. In Figure 1(b), the region around the Sm-Co(11–20) peak is shown, for films grown with a sputter pressure of 1.5, 3.0, 7.5, and 10.5×10^{-3} mbar. Clearly visible is that, with decreasing pressure, the peaks shift to a higher angle. The measured lattice constant, determined from the Sm-Co(22–40) peak, and the Sm content, determined by RBS, are plotted in Figure 2 as a function of the sputter pressure. For films grown at a pressure above 6.0×10^{-3} mbar, the lattice parameter of the Sm-Co film is almost that of bulk Sm_2Co_7 (0.5040 nm). Decreasing the pressure from 6.0×10^{-3} mbar shows a decreasing lattice parameter, and at the lowest pressure the lattice constant of the Sm-Co film almost reaches the $SmCo_5$ bulk value (0.4982 nm). With respect to the Sm concentration, we consistently find a somewhat higher number than the stoichiometric Sm-Co phases would yield. Above 6.0×10^{-3} mbar, the Sm concentration is around 25–27 at. % (compared to 22 at. % for Sm_2Co_7). Below 6.0×10^{-3} mbar, the Sm content gradually decreases to 21 at. % (compared to 17 at. % for $SmCo_5$).

Figures 3(a)–3(d) show the morphology of the Sm-Co films grown at 1.5, 3.0, 7.5, and 10.5×10^{-3} mbar, respectively. The films grown at a high sputter background pressures consist of rectangular grains with an average size of 70×250 nm^2, and with the long axis distributed over the two orthogonal directions MgO[100] and MgO[010]. Statistical analysis over an area of $1 \times 1\ \mu$m^2 on a Sm-Co film grown at 7.5×10^{-3} mbar indicates an average surface roughness of 6.0 nm and a peak to peak value of 67 nm. When decreasing the pressure below 6×10^{-3} mbar, the shape of the grains slowly transforms from rectangular to square-like. Sm-Co films grown at 1.5×10^{-3} mbar consist of square grains with an average size of 75×75 nm^2. Statistical analysis over an area of $1 \times 1\ \mu$m^2 on the Sm-Co film grown at 1.5×10^{-3} mbar indicates an average surface roughness of 9.6 nm and a peak to peak value of 55 nm.

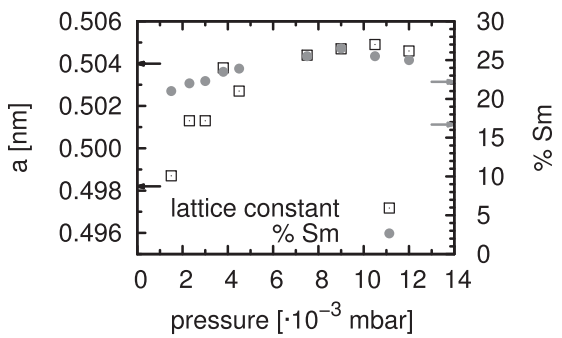

FIG. 2. Lattice constant a of Sm-Co films and Sm concentration in the films as a function of the sputter background pressure, where the black (←) and red (→) arrows indicate the lattice constant and Sm concentration of bulk $SmCo_5$ and Sm_2Co_7. Clearly visible is the change of the lattice parameter a from the Sm_2Co_7 phase ($a = 0.5040$ nm) to the $SmCo_5$ phase ($a = 0.4982$ nm).

B. Magnetic properties at room temperature

In Figure 4, the magnetization measurements are shown, taken at room temperature. The magnetization was calculated by dividing the measured magnetic moment by the

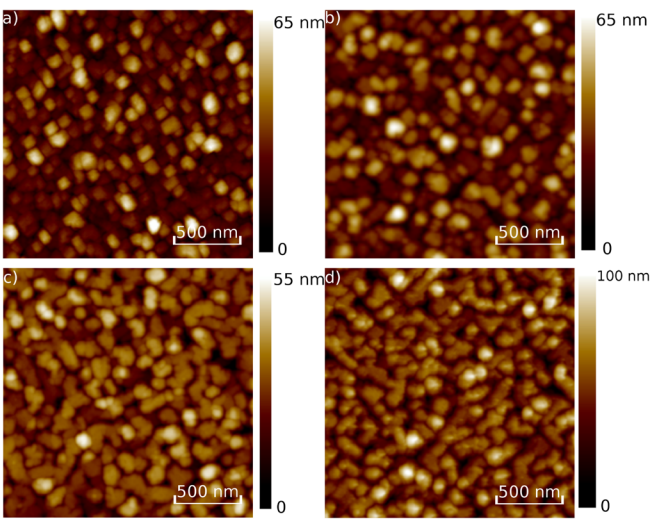

FIG. 3. Morphology of Sm-Co films grown at (a) 1.5×10^{-3}, (b) 3×10^{-3}, (c) 7.5×10^{-3}, and (d) 10.5×10^{-3} mbar measured with atomic force microscopy.

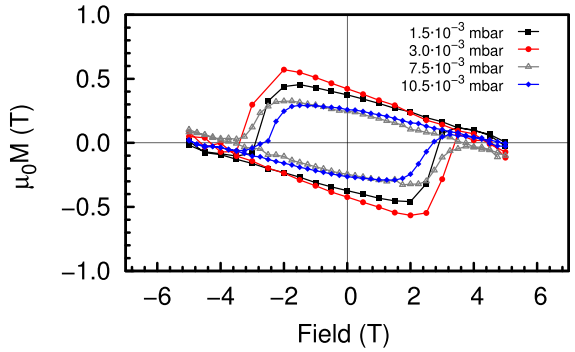

FIG. 4. Magnetization M as function of magnetic field at 300 K for Sm-Co films on a Cr/MgO(100) substrate grown with different sputter gas pressures as indicated.

measured volume of the Sm-Co films (typically, 10 mm × 4 mm × 100 nm, where the Sm-Co thickness was determined using RBS). All samples show hysteretic behavior with a square-like loop and a large coercivity, of the order of 3 T, but also a substantial diamagnetic contribution. Separate measurements on a MgO(100) substrate and a MgO(100)/Cr(100 nm)/Cu(30 nm) film show that, at room temperature, the magnetic susceptibility χ of MgO for substrates from different batches varied and the samples measured had a magnetic susceptibility of -2.4 and -3.5×10^{-7} emu/g. These values are in agreement with $\chi = -5.1 \times 10^{-7}$ emu/g for a single crystal of MgO.[22]

For the films grown at 1.5, 3.0, and 10.5×10^{-3} mbar, the coercive fields H_c are 2.6, 3.0, and 2.1 T and the remanent magnetization $\mu_0 M_{rem}$ are 0.4, 0.4, and 0.3 T. Both $\mu_0 H_c$ and $\mu_0 M_{rem}$ as a function of sputter pressure are given in Figure 5. Again we find clear trends: with increasing pressure up to 6×10^{-3} mbar $\mu_0 H_c$ slowly increases from 2.6 T to 3.3 T, but above 6×10^{-3} mbar a rapid decrease sets in, down to 1.8 T at 12×10^{-3} mbar. The remanent magnetization is 0.4 T–0.2 T in the whole pressure range. To characterize the magnetic texture, the ratio of the remanence of the in-plane and out-of-plane magnetization was determined for the film grown at 1.5×10^{-3} mbar (not shown). These data show that such a film has a preferred in-plane orientation of the easy axis. One single exception in the dataset was a film grown at 6.0×10^{-3} mbar, for which we found a remanent magnetization of 0.9 T. Since such a value is difficult to explain, and since morphology and lattice parameters for the film showed normal values, we chose not to consider or show other data from that sample.

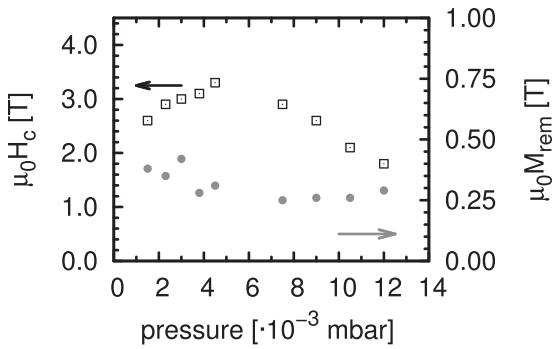

FIG. 5. The coercive field H_c and the remanent magnetization M_{rem} at 300 K of the Sm-Co films as a function of the sputter background pressure.

C. Target variability

One issue which came up during the research is target variability. We have grown Sm-Co films using a number of different commercially obtained targets with requested composition $SmCo_5$, which, according to the vendor, where fabricated from the same batch of alloy material. In Figure 6, the pressure dependence of the lattice constant of the Sm-Co films grown with three different targets is shown. The data discussed above were from films grown with target 1. Clearly visible is that the lattice parameters and therefore the exact film composition varies for the different targets. For target 2, the lattice parameters do not decrease when going to low pressure, which indicates a slight excess of Sm with respect to target 1. Films from target 3 show a considerably lower lattice parameter (typically 1%) and apparently contain much more Co, although the lattice parameter is still lower than what is expected for the Sm_2Co_{17} compound (0.419 nm). ICP analysis of the three targets showed the target bulk composition to be $SmCo_{4.56}$ (target 1), $SmCo_{4.62}$ (target 2), and $SmCo_{4.63}$ (target 3), which means the targets were very similar in composition. However, the films grown with targets 2 and 3 showed coercive fields which were generally lower, between 1.0 and 2.0 T. The reason for this variability is not clear, but it possibly to be found in composition changes at the target surface due to the high temperature of the target during the sputtering process. We did not attempt to optimize the magnetic properties by varying the growth temperature.

D. Magnetic properties at low temperatures

We also investigated the low temperature behavior of the Sm-Co films. In Figure 7, the uncorrected magnetization hysteresis loops for a Sm-Co film grown at 10.5×10^{-3} mbar are shown as a function of temperature. For the temperatures of 70 K and below, the magnetization loops are fully hysteretic between +5 T and −5 T, indicating that the coercive field has increased to above 5 T and only minor loops are now being measured. Also, the diamagnetic contribution of

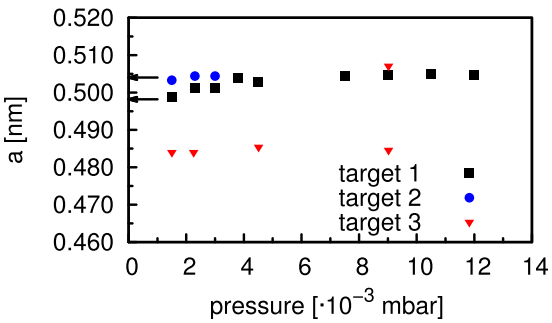

FIG. 6. The lattice constant a of the Sm-Co films, grown with three different composite targets, which were fabricated from the same batch of alloy material, as a function of the sputter background pressure. The black (←) arrows indicate the lattice constant of bulk $SmCo_5$ and Sm_2Co_7. The two lattice constants at 9.0×10^{-3} mbar for target 3 indicates that there are two phases present in the film.

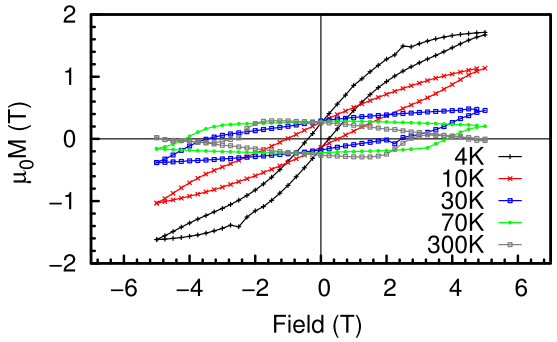

FIG. 7. (a) Magnetization M as function of magnetic field of the Sm-Co film grown at 10.5×10^{-3} mbar as a function of temperature. For the 10 K and 4 K loop, the 5 T magnet of the magnetometer is not strong enough to reach the coercive field of the Sm-Co film while the contribution of the MgO substrate increases significantly.

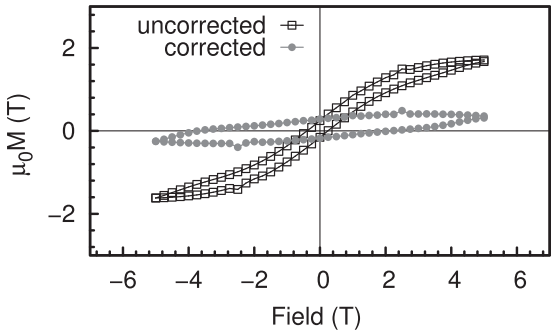

FIG. 9. Magnetization M as function of magnetic field (black squares) of a Sm-Co film grown at 10.5×10^{-3} mbar. The measurement is at 4.2 K. The gray dots are the values for M after correction for the substrate contribution. A small hysteresis characteristic of a minor loop is visible.

the substrate becomes smaller. When going to even lower temperatures, the hysteresis loop shows a clear paramagnetic behavior. Figure 8(a) shows magnetization measurements at 4 K for two virgin (no pretreatment, no heating) MgO substrates from different batches, which are clearly paramagnetic in character. EPR measurements were done to identify the paramagnetic impurities. Figure 8(b) shows the room temperature EPR measurements of a MgO substrate. Clearly visible are the resonance lines of Cr^{3+}, V^{2+}, and Mn^{2+} impurities.[23] In Figure 9, the uncorrected and corrected magnetization hysteresis loops at 4.2 K for a Sm-Co film grown at 10.5×10^{-3} mbar are shown. The corrected hysteresis loop can be seen to be a minor loop without clear switching when reversing the field direction, and asymmetry with respect to the positive and negative zero-field magnetization. It shows that the coercive field is larger than 5 T.

V. DISCUSSION

Summarizing the experimental findings for target 1, we see that, when varying the sputter background pressure between 1.5×10^{-3} and 12.5×10^{-3} mbar, the Sm concentration in the films varies between 21 and 26.5 at. %. In the whole pressure range, we find the Sm content of the films higher than expected from the stoichiometric ratios of the line compounds. The films are not a mixture of the $SmCo_5$ and Sm_2Co_7 compounds, which would result in two lines with different weight in the X-ray data. Rather, the films consist of one main composition which is able to incorporate a varying amount of Co-atoms. This is in line with the picture of Kahn,[24] who proposed that the crystal structure of the intermetallic compounds can be seen as a one-dimensional superstructure of the $CaCu_5$-type structure, where in each i-th $CaCu_5$-type structure a Co-atom is replaced by a Sm-atom. Khan described this structure with the general formula $SmCo_y$, where y is equal to $(5n+4)/(n+2)$ (with n an integer). According to the XRD data, at the lowest pressure the films are close to the $SmCo_5$ compound, going to Sm_2Co_7 at higher pressures. With increasing sputter pressure, both the lattice constant and the value for H_c increases until the pressure of 6.0×10^{-3} mbar is reached, where the lattice parameter corresponds to the Sm_2Co_7 alloy (although still with Sm excess). At the same time, M_{rem} slowly decreases from about 0.4 T to 0.3 T. Increasing the pressure further, H_c starts to decrease while M_{rem} becomes constant. The surface morphology in Figure 3 shows that the grain size and grain shape changes when the sputter pressure is changed. At high pressures, relatively large rectangular grains are grown. When reducing the pressure, the grains become smaller and more square-like. We surmise this is due to the change in average energy of the atoms bombarding the substrate: at low pressure, this energy is higher and as a result, more defects are created during the growth of the first Sm-Co layers. When the number of defects becomes larger, also the number of preferred nucleation sites increases. The increase in the number of nucleation sites results in a reduced grain size and a more rough surface. Connecting the structure/morphology

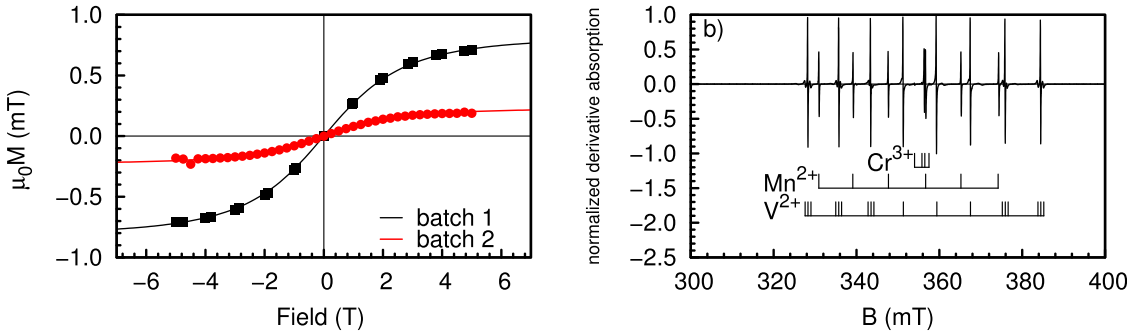

FIG. 8. (a) Magnetization M as function of magnetic field for two MgO substrates from different batches measured at 4 K. The solid lines are fits to a Brillouin function using Cr^{3+}, Mn^{2+}, and V^{2+} impurities. (b) A typical room temperature EPR spectrum of a MgO single crystal substrate containing Cr^{3+}, Mn^{2+}, and V^{2+} impurities.

data to the magnetization data, we see that in the range of pressures where the films change from $SmCo_5$-like to Sm_2Co_7-like, the values of H_c (2.6 T–3.3 T) and M_{rem} (0.4 T–0.3 T) are the highest, and in particular H_c is close to what has been achieved with cosputtering. M_{rem} is lower than optimal. For an equal distribution of two easy axes, the expected value is $M_s/\sqrt{2}$, or 0.78 T both for $SmCo_5$ and for Sm_2Co_7.[25] This is in agreement with Ref. 8, where it was shown that excess of Sm leads to a significant decrease of M_{rem}. The films grown above 6.0×10^{-3} mbar show a decrease in coercive field, although the Sm concentration, lattice constant and remanent magnetization do not change significantly with respect to the films grown at lower pressures. We attribute the change in coercive field to the larger grain size of the grown Sm-Co film. In experiments with nanoparticles with a different size, it was found that the size has a significant influence on the coercive field and an optimum particle size is approximately 100–200 nm.[26]

At low temperatures, the picture is somewhat complicated by the paramagnetic behavior of the MgO substrates, which is due to transition metal impurities, in particular, Mn, V, and Cr. Their amount varies from batch to batch. Up to now, not much attention has been paid to the influence of the transition metal impurities on the properties of the grown films. Recently, the influence of the transition metal impurities on the optical and magnetic properties of a bare MgO substrate was studied.[27] Since the low temperature magnetic hysteresis shows a clear paramagnetic behavior superimposed on it, we assume that the magnetization M_{imp} of these impurities can be described by the Brillouin function

$$M_{\mathrm{imp}} = NgJ\mu_B \frac{2J+1}{2J} \coth\left(\frac{2J+1}{2J}\frac{gJ\mu_B JB}{k_b T}\right) - NgJ\mu_B \frac{1}{2J} \coth\left(\frac{1}{2J}\frac{gJ\mu_B JB}{k_b T}\right), \quad (1)$$

with N is the number of atoms, g is the g-factor, μ_B is the Bohr magneton, J is the total angular momentum, k_B is the Boltzman constant, and T is the temperature. The total magnetization for the three different impurities is then modeled as the sum of the magnetization of each type of impurities. From fitting Eq. (1) to the low temperature magnetization of a bare MgO substrate, we estimate that in the MgO substrates in Figure 8(a), the concentration of the impurities is in the range of 15–60 ppm.[27] When the contribution of the impurities in the MgO substrate is subtracted using Eq. (1), the Sm-Co film yields a hysteresis loop as shown in Figure 9. It is a minor loop, as discussed above, since the coercive field is larger than the 5 T which can be reached in the magnetometer.

VI. CONCLUSION

When growing SmCo films from a single target with the nominal composition of $SmCo_5$ target on a Cr-buffered MgO(100) substrate, high coercive fields can be reached, up to 3.3 T. In order to avoid low remanence, excess Sm has to be avoided. Although, in principle, the Sm content can be varied using the sputter pressure, the amount of control depends on the sputtering configuration. In the case described here, the lowest pressure at which we could grow films appears to be too high for this goal, in particular, since the target was slightly Sm-rich to start with. A Co-rich target might be a solution for this problem. Whether that would solve the other difficulty we encountered, namely, the high sensitivity of the film properties to different targets of nominally the same composition is an open question. That sensitivity is certainly a hindrance, since it requires relatively costly optimization of the deposition conditions for each target separately. At low temperatures, we achieved the high coercive fields characteristic for these hard magnetic materials, but we also found that the data are strongly dominated by paramagnetic impurities in the MgO substrates.

ACKNOWLEDGMENTS

We thank Roger Wördenweber and Eugen Hollmann at the Forschungszentrum Jülich for the RBS measurements. Financial support from the European Commission (FP7-ICT-FET No. 225955 STELE) is gratefully acknowledged.

[1]T. S. Chin, "Permanent magnet films for applications in microelectromechanical systems," J. Magn. Magn. Mater. **209**(13), 75–79 (2000).
[2]S. Sawatzki, R. Heller, Ch. Mickel, M. Seifert, L. Schultz, and V. Neu, "Largely enhanced energy density in epitaxial $SmCo_5$/Fe/$SmCo_5$ exchange spring trilayers," J. Appl. Phys. **109**(12), 123922 (2011).
[3]J. Engelmann, T. Shapoval, S. Haindl, L. Schultz, and B. Holzapfel, "Growth and characterization of NbN/$SmCo_5$ bilayers: The influence of magnetic stray field on the upper critical field of the superconductor," J. Phys.: Conf. Ser. **234**(1), 012012 (2010).
[4]H. Okamoto, "Co-Sm (cobalt-samarium)," J. Phase Equilib. **20**, 535–536 (1999).
[5]A. Singh, V. Neu, S. Fähler, K. Nenkov, L. Schultz, and B. Holzapfel, "Mechanisms of coercivity in epitaxial $SmCo_5$ thin films," Phys. Rev. B **77**(10), 104443 (2008).
[6]L. N. Zhang, J. S. Chen, J. Ding, and J. F. Hu, "High-coercivity $SmCo_5$ thin films deposited on glass substrates," J. Appl. Phys. **103**(11), 113908 (2008).
[7]A. Singh, V. Neu, R. Tamm, K. Subba Rao, S. Fähler, W. Skrotzki, L. Schultz, and B. Holzapfel, "Growth of epitaxial $SmCo_5$ films on Cr/MgO(100)," Appl. Phys. Lett. **87**(7), 072505 (2005).
[8]A. Singh, V. Neu, S. Fähler, L. Schultz, and B. Holzapfel, "Effect of composition on phase formation and magnetic properties of highly coercive SmCo films," J. Magn. and Magn. Mater. **290–291**, 1259–1262 (2005).
[9]R. Tamm, K. S. Rao, S. Fähler, V. Neu, A. Singh, C.-G. Oertel, L. Schultz, B. Holzapfel, and W. Skrotzki, "Texture formation in epitaxial hard magnetic Sm_2Co_7 thin films," Phys. Status Solidi A **207**(1), 106–116 (2010).
[10]E. E. Fullerton, C. H. Sowers, J. P. Pearson, S. D. Bader, X. Z. Wu, and D. Lederman, "A general approach to the epitaxial growth of rare-earth-transition-metal films," Appl. Phys. Lett. **69**(16), 2438–2440 (1996).
[11]L. N. Zhang, J. F. Hu, J. S. Chen, and J. Ding, "Nanostructured $SmCo_5$ thin films with perpendicular anisotropy formed in a wide range of SmCo compositions," J. Nanosci. Nanotechnol. **11**(3), 2644–2647 (2011).
[12]F. J. Cadieu, "Selectively thermalized sputtering for the deposition of magnetic films with special anisotropies," J. Vac. Sci. Technol., A **6**(3), 1668 (1988).
[13]V. Neu and S. A. Shaheen, "Sputtered Sm–Co films: Microstructure and magnetic properties," J. Appl. Phys. **86**(12), 7006–7009 (1999).
[14]R. Andreescu and M. J. O'Shea, "Temperature dependence of coercivity and magnetic reversal in $SmCo_x$ thin films," J. Appl. Phys. **97**(10), 10F302 (2005).
[15]G. Zangari, B. Lu, D. E. Laughlin, and D. N. Lambeth, "Structure and magnetic properties of SmCo thin films on Cr/Ag/Si templates," J. Appl. Phys. **85**(8), 5759–5761 (1999).
[16]T. Speliotis and D. Niarchos, "Microstructure and magnetic properties of SmCo films," J. Magn. Magn. Mater. **290–291**, 1195–1197 (2005).
[17]L. Peng, H. Zhang, Q. Yang, Y. Li, Y. Song, and J. Shen, "Correlation between sputtering parameters and composition of SmCo-based films for

microelectromechanical system applications," J. Appl. Phys. **105**(6), 063915 (2009).
[18]J. Y. Wang, M. K. Ghantasala, and R. J. McLean, "Bias sputtering effect on ultra-thin $SmCo_5$ films exhibiting large perpendicular coercivity," Thin Solid Films **517**(2), 656–660 (2008).
[19]G. Xue, L. Peng, and H. Zhang, "Effect of sputtering parameters on film composition, crystal structure, and coercivity of SmCo based films deposited on Si (100) substrates," Chin. Phys. Lett. **27**(1), 017501 (2010).
[20]F. J. Cadieu, H. Hegde, and K. Chen, "High-energy product Sm-Co-based sputtered films, crystal texturing, and magnetic properties," J. Appl. Phys. **67**(9), 4969–4971 (1990).
[21]E. E. Fullerton, J. S. Jiang, C. Rehm, C. H. Sowers, S. D. Bader, J. B. Patel, and X. Z. Wu, "High coercivity, epitaxial SmCo films with uniaxial in-plane anisotropy," Appl. Phys. Lett. **71**(11), 1579–1581 (1997).
[22]B. L. Gordon and M. S. Seehra, "Magnetic susceptibility of Mn^{2+} ions in MgO and evidence of clustering," Phys. Rev. B **40**, 2348–2353 (1989).
[23]J. S. van Wieringen and J. G. Rensen, "Influence of lattice imperfections on the paramagnetic resonance of V^{2+} and Cr^{3+} in MgO," in *Paramagnetic Resonance*, edited by W. Low (Academic Press, New York, 1963), Vol. 1, pp. 105–112.
[24]Y. Khan, "Variation of period with valence electron concentration in RT_y one-dimensional long-period superstructures," Phys. Status Solidi A **23**(2), 425–434 (1974).
[25]M. I. Bartashevich, A. V. Andreev, E. N. Tarasov, T. Goto, and M. Yamaguchi, "Magnetic properties and spontaneous magnetostriction of a Sm_2Co_7 single crystal," Physica B **183**, 369–378 (1993).
[26]C. H. Chen, S. J. Knutson, Y. Shen, R. A. Wheeler, J. C. Horwath, and P. N. Barnes, "The effect of particle size on coercivity and crystallinity of SmCo–5," Appl. Phys. Lett. **99**(1), 012504 (2011).
[27]S. Prucnal, A. Shalimov, M. Ozerov, K. Potzger, and W. Skorupa, "Magnetic and optical properties of virgin arc furnace grown MgO crystals," J. Cryst. Growth **339**(1), 70–74 (2012).